Supporting online material

Experimental details: Aqueous solutions are pumped (50 μL min^{-1}, Harvard Apparatus) into the spraying chamber of a commercial ESMS instrument (Agilent HP-1100 MSD) through a grounded stainless steel needle injector (100 μm bore) and pneumatically nebulized by means of N_2 gas flowing through a coaxial sheath.[1] The difference between the exit velocities of the liquid jet (10.6 cm s^{-1}) and nebulizer gas (2.65×10^4 cm s^{-1}) is so large that the drag imposed on the liquid breaks it apart into sub-micrometer size droplets. The terminal velocities of the microdroplets thus produced exceed ~10^3 cm s^{-1} [2] which lead to transit times shorter than $\tau \sim$ 1 ms across the ~ 0.5 cm wide O_3(g) plume. These droplets, which are produced by fragmentation of electrically neutral solutions from a grounded injector, are charged via statistical fluctuations that scale with (drop size)$^{-1/2}$.[3] The ensemble of spray droplets is on average neutral, but individual droplets actually carry charges that follow a Gaussian distribution, as expected for a random process. This phenomenon is the basis of the classical oil drop experiment performed by Millikan to determine the magnitude of the elementary charge.[4] It should be emphasized that spontaneous, asymmetrical charge separation during pneumatic nebulization of liquids does not produce highly charged droplets and, therefore, it is unrelated to electrospray ionization of droplets issuing from high-field nozzles. Sprayed droplets eventually contract via solvent evaporation, a process regulated by ambient temperature and relative humidity, thereby increasing electrostatic repulsion among excess surface charges. Coulomb explosions ensue in which drops shed interfacial charge and mass into smaller droplets. In the final stage, ions are ejected from nanodroplets into the gas-phase.[5-7] It is apparent that, by its very nature, this technique effectively samples the interfacial layers of nanodroplets. Product identities were confirmed via MS-MS analyses performed in an Agilent MSD-Trap mass spectrometer.

Ozone is generated by flowing ultrapure O_2(g) (Air Liquide) through a commercial

ozonizer (Ozone Solutions, Inc.), diluted tenfold with ultrapure N_2(g), and quantified by UV absorption spectrophotometry (HP 8452) at 250 and 300 nm prior to entering the spraying chamber, where it contacts the aqueous UA droplets for ~ 1 millisecond. This arrangement has been described and illustrated in detail elsewhere.[1] Throughout, the reported [O_3(g)] values, which correspond to the concentrations actually sensed by microdroplets in the reaction chamber, are estimated to be ~10 times smaller than the values determined from UV absorbances due to further dilution by the N_2 drying gas. Gas flows were regulated by calibrated mass flow controllers (MKS). Typical instrumental parameters were as follows: drying gas temperature, 250 ^{o}C; Nebulizer pressure, 28 psi; collector capillary voltage, +3.5 kV; fragmentor voltage, 17 V. Evidence that droplets are charged via statistical charge separation rather than by electrical field effects under present conditions is shown previously,[1] where we showed that the kinetics of I^- oxidation by O_3(g) was unaffected by changing the collector capillary voltage from +1.5 to +3.5 kV relative to ground, i.e., to the needle injector. Solutions were prepared in MilliQ water, or in D_2O (D > 99.9%, Cambridge Isotope Laboratories). Natural abundance uric acid (Aldrich) and [1,3-$^{15}N_2$] uric acid (Cambridge Isotope Laboratories, > 98 %), *tert*-butanol (Fisher) and H_2O_2 (Fisher) were used as received. Solutions pH was adjusted by HCl (VWR) and NaOH (J. T. Baker) and measured with a calibrated pH meter (VWR).

Appendix 1: Reactant diffusion from the droplets core may account for the leveling off, i.e., the weaker than exponential decay of $[U^-]/[U^-]_0$ vs. [O_3(g)] (Fig. 3, lower left panel). If the concentration of $X \equiv U^-$ in the interfacial layers is determined by its reaction with O_3(aq) $\rightleftharpoons$ O_3(g), and by diffusion from the droplets core, then:

$$\frac{\partial[\mathrm{X}]}{\partial t} = \frac{D}{\delta}\frac{[\mathrm{X}]_0 - [\mathrm{X}]}{\Delta} - k[\mathrm{O_3}]\,[\mathrm{X}]\,; \qquad D' \equiv \frac{D}{\delta\,\Delta} \qquad \text{(SE1)}$$

$$[\mathrm{X}] = \frac{D'[\mathrm{X}]_0 - k[\mathrm{O_3}]\,[\mathrm{X}]_0 \exp[-(D' + k[\mathrm{O_3}])t]}{D' + k[\mathrm{O_3}]} \qquad \text{(SE2)}$$

$$\frac{[\mathrm{X}]_{ss}}{[\mathrm{X}]_0} = \frac{D'}{D' + k[\mathrm{O_3}]} \qquad \text{(SE3)}$$

$$\frac{\partial([\mathrm{X}]_{ss}/[\mathrm{X}]_0)}{\partial[\mathrm{O_3}]} \;\rightarrow\; -\frac{k}{D'} \quad \text{as} \;\; [O_3] \rightarrow 0 \qquad \text{(SE4)}$$

where D is the diffusion coefficient of X in water, δ is the thickness of the interfacial shell, and Δ the length over which its intradroplet concentration gradient is established. k is the local (X + O_3) reaction rate constant in the interfacial layers. The solution of SE1 is given by SE2. In the absence of diffusion, i.e., $D' = 0$, [X] decays exponentially with time, at constant [O_3]. However, since X can diffuse (with $D \sim 2 \times 10^{-5}$ cm^2 s^{-1}) in tens of nanoseconds through, say, a $\Delta \sim 10$ nm layer, a stationary state should be rapidly established within the ~ 1 ms timeframe of our experiments. This condition is encoded by equation SE3, the limiting form of SE2 at $t \rightarrow \infty$. By assuming, as a first approximation, that D' is constant, the $[X]_{ss}/[X]_0$ ratio becomes an inverse rational function of [O_3] at constant contact time. The initial slope, given by SE4, is therefore proportional to the reaction rate constant k. Plots calculated from SE3 for various parameter combinations (Fig. S1) show that $[X]_{ss}/[X]_0$ indeed "levels off" at large [O_3(g)], supporting our interpretation of this phenomenon. A more realistic analysis should deal with the development of intradroplet concentration gradients as functions of time, radius and [O_3(g)] (8), but it is doubtful that classical continuum diffusion models will be adequate for this task. The leveling off of experimental $[U^-]/[U^-]_0$ vs. [O_3(g)] curves cannot be due to diffusional limitations in the gas-phase because this event is not replicated in the ozonolysis of other anions, such as $S_2O_3^{\cdot-}$ or I^-, over the same [O_3(g)] ranges in 1 atm N_2(g) (1). Note that, since intradroplet diffusion contributes significantly to monitored interfacial [X] concentrations, interfacial layers behave as open reactors in which formal product P

yields calculated as: $Y_P = ([P]_f - [P]_0)/([X]_0 - [X]_f)$ may exceed unity (1, 9). Conventional integrated kinetic equations for closed, well-mixed chemical reactors are, of course, inapplicable to interfacial layers.

Captions to figures

Figure S1: $[U^-]/[U^-]_0$ vs. $[O_3(g)]$ plots calculated from equation SE3 using the parameters reported in the plot to illustrate the effects of reaction and diffusion on U^- decay kinetics.

Figure S2: Schematic diagram of continuous flow T-mixer setup used to study the reaction between UA and O_3. 0.2 mM aqueous UA solutions at pH 3.6 to 10.3 and O_3-sparged water are pumped through the T-mixer into the ES.

Figure S3: Upper panel: ESMS of 0.2 mM uric acid at pH = 6.6. Lowe panel: ESMS of the products of mixing 0.2 mM aqueous UA solutions pH 6.6 with O_3-sparged water in the T-mixer shown in Fig. S2 after 24 s contact time.

Figure S4: U^- decay in the ozonolysis of 0.2 mM UA microdroplets as a function of $[O_3(g)]$ in the absence (blue) / presence (red) of 1.1 M *tert*-butanol at pH = 7.6.

Figure S5: Urate and products of the ozonolysis of 0.2 mM UA microdroplets at pH7.6 as functions of $[O_3(g)]$ in the absence (blue circles) / presence (red triangles) of 0.4 M H_2O_2.

Figure S6: ($(U\text{-}O)^-$ (circle), $(U\text{-}O_2)^-$ (triangle) and $(U\text{-}O_3)^-$ (square) yields based on interfacial urate losses as a function of bulk pH. Yields (Y) defined in terms of signal intensities (S) as $Y(X) = [S(X^-)]/ [S(U_0^-) - S(U^-)]$ on the assumption of identical response factors. Note the 10 × amplification of Y $(U\text{-}O_2)^-$.

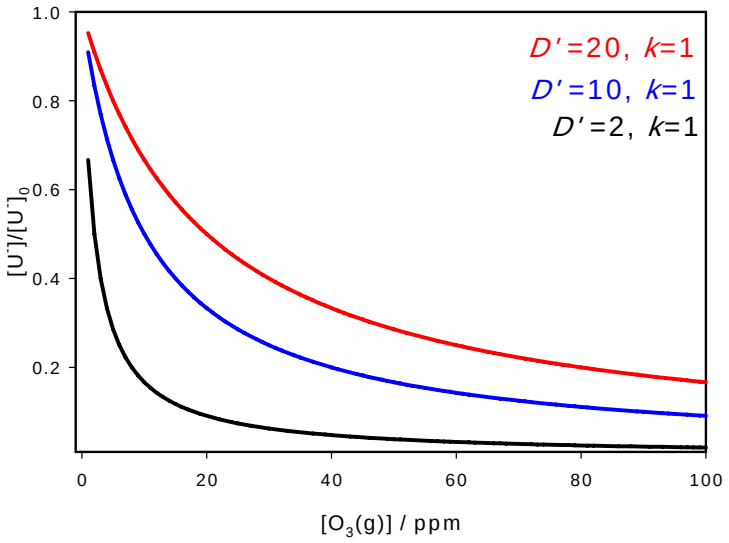

Figure S1

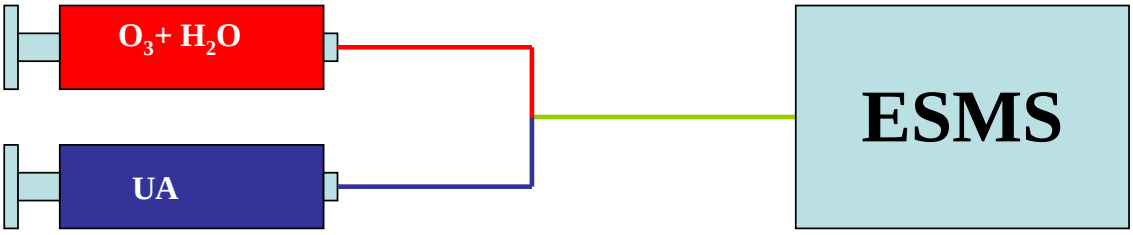

Figure S2

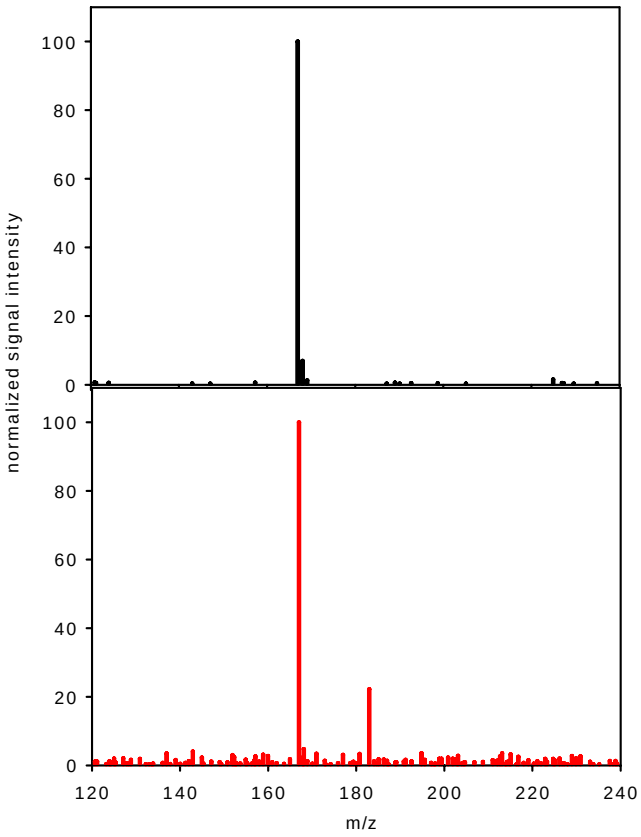
normalized signal intensity
100
80
60
40
20
0
100
80
60
40
20
0
120
140
160
180
200
220
240
m/z

Figure S3

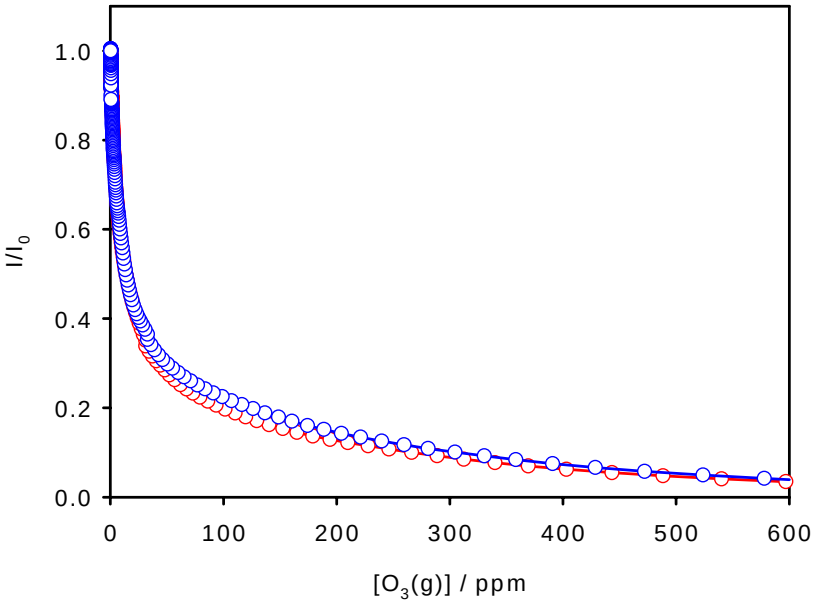

Figure S4

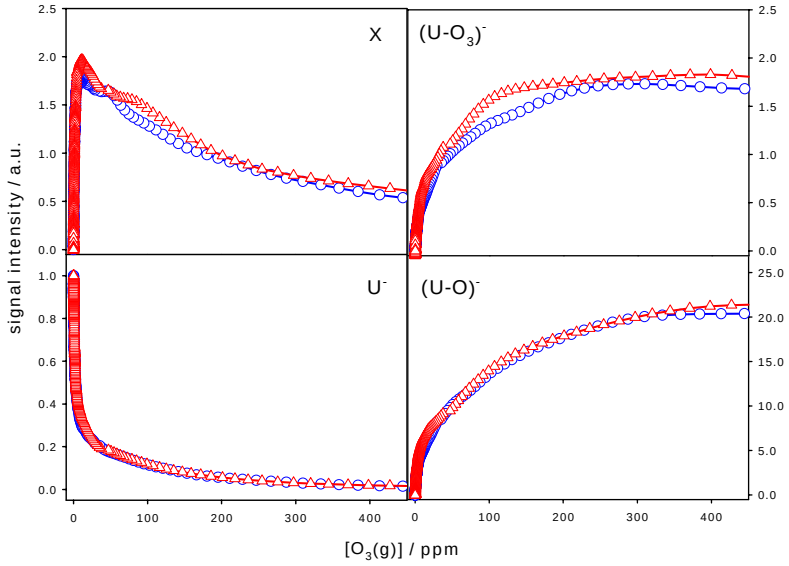

Figure S5

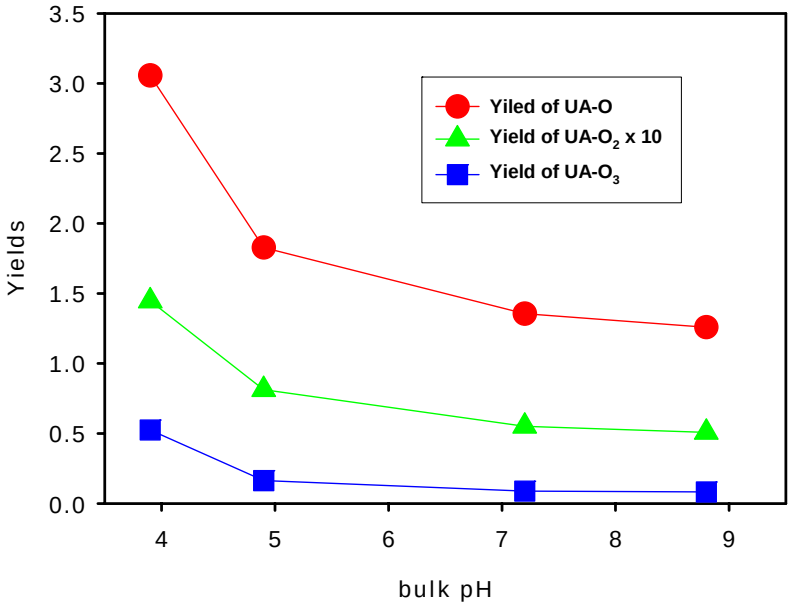
3.5
3.0
2.5
2.0
1.5
1.0
0.5
0.0
Yields
4
5
6
7
8
9
bulk pH
Yiled of UA-O
Yield of UA-O2 x 10
Yield of UA-O3

Figure S6

References

1. Enami, S.; Vecitis, C. D.; Cheng, J.; Hoffmann, M. R.; Colussi, A.J. *J. Phys. Chem. A* **2007**, *111*, 8749.
2. Kahen, K.; Jorabchi, K.; Gray, C.; Montaser, A. *Anal. Chem.* 2004, 76, 7194.
3. Dodd, E. E. *J. Appl. Phys.***1953**, *24*, 73.
4. Millikan, R. A. *Science* **1910**, *32*, 436.
5. Fenn, J. B. *J. Am. Soc. Mass Spectrom.* **1993**, *4*, 524.
6. Kebarle, P.; Tang, L. *Anal. Chem.* **1993**, *65*, 972.
7. Kebarle, P. Peschke, M. *Analytica Chimica Acta* **2000**, *406*, 11.